

# Nanoelectrodes, nanoelectrode arrays and their applications†

**Damien W. M. Arrigan**

*Chemical MicroAnalytics, NMRC, University College, Lee Maltings, Prospect Row, Cork, Ireland. E-mail: damien.arrigan@nmrc.ie; Fax: +353-21-4270271; Tel: +353-21-4904079*

*Received 4th October 2004, Accepted 1st November 2004*

*First published as an Advance Article on the web 9th November 2004*

This review deals with the topic of ultrasmall electrodes, namely nanoelectrodes, arrays of these and discusses possible applications, including to analytical science. It deals exclusively with the use of nanoelectrodes in an electrochemical context. Benefits that accrue from use of very small working electrodes within electrochemical cells are discussed, followed by a review of methods for the preparation of such electrodes. Individual nanoelectrodes and arrays or ensembles of these are addressed, as are nanopore systems which seek to emulate biological transmembrane ion transport processes. Applications within physical electrochemistry, imaging science and analytical science are summarised.

## Introduction

Ultrasmall electrodes (micrometre size or smaller) offer a number of advantages when employed in electrochemical studies and applications. The benefits which accrue from these, also known as microelectrodes or ultramicroelectrodes,<sup>1–5</sup> can be expected to be achieved to a greater extent with nanoelectrodes. Thus enhanced mass transport, due to dominance of radial diffusion, decreased charging currents and decreased deleterious effects of solution resistance, can all be expected with nanoelectrodes and enable new applications of ultrasmall electrochemical systems. Nanoelectrodes may be defined as electrodes with a critical dimension in the nanometre range, where by critical dimension is meant that dimension which controls the electrochemical response. Thus any sub-micrometre electrode can be viewed as a nanoelectrode. On the otherhand, a microelectrode or ultramicroelectrode may be viewed as any electrode in which the electrode is smaller in

magnitude than the diffusion layer which can be achieved in an experiment, yielding an electrode with a critical dimension (*e.g.* radius) of the order of 25  $\mu\text{m}$ . When the electrode's critical dimension is further decreased to the same order as the thickness of the electrical double layer or the molecular size, the experimental behaviour starts to deviate from extrapolations of behaviour at larger electrodes. This point may be viewed as the separation point between nanoelectrodes (or nanodes) and microelectrodes.<sup>4</sup> Generally, in keeping with other aspects of nanoscience and nanotechnology, in which the length scale of interest is the range 1–100 nm, the critical dimension of nanoelectrodes can be taken as being in that range too. As will be seen in the following sections, many electrodes fall within this range, including some below it, but there are assumptions made in reaching the obtained critical dimension values. One of the main driving forces for development of nanoelectrodes has been to achieve electrodes whose critical dimension (*i.e.* radius for a disc or hemisphere, width for a band) is similar to molecular dimensions. At the present state of development of nanoelectrodes, which this paper reviews, the main issues facing nanoelectrodes are preparation of devices and understanding of their electrochemical performance. Although a number of applications have begun to appear, this area is still very much in its infancy.

The paper reviews the current state of the art in the fabrication of both individual nanoelectrodes and nanoelectrode arrays or ensembles. Individual nanoelectrodes, and collections of individual nanoelectrodes, whether arranged in an orderly array or randomly dispersed throughout an inert matrix, are considered. The area has been researched through use of on-line databases (such as the Web of Science<sup>®</sup> of the Institute for Scientific Information) and browsing of journal contents pages. The review reflects each of the current areas of endeavour in research related to nanoelectrodes. However, nanostructured materials<sup>7</sup> and densely-packed or random collections of carbon nanotubes (CNTs)<sup>8</sup> are omitted. Up-to-date information on those materials is available elsewhere. The concentration on individual and arrayed nanoscale electrodes is based on the electrochemical behaviour observed rather than on the structure of the material used.

The format of the paper follows logically from why nanoelectrodes might be of interest, through how they can be prepared and their electrochemical properties, to applications of nanoelectrodes. A brief glimpse into the related area of sensing based on ion movement through nanopores is also presented.

*Damien Arrigan is a senior research scientist and Team Leader—Chemical MicroAnalytics at NMRC, University College, Cork, Ireland. His research interests are in the combination of electrochemical processes with micro- and nano-systems technology for the development of biologically-inspired molecular measurement strategies. He studied Analytical Science (BSc) at Dublin City University and worked in the biotechnology industry in Ireland before studying for his PhD in Analytical Chemistry at University College, Cork, with Prof. Gyula Svehla. After postdoctoral work at NMRC and at the University of Southampton, and a lectureship at the University of Salford 1995–2001, he returned to Cork to his present position. The Royal Society of Chemistry—Analytical Division awarded him its SAC Silver Medal in 2001.*



† Presented at the Symposium on “Nanotechnology: Surfaces, Sensors and Systems” at the 10th International Conference on Electroanalysis, June 6–10, 2004, Galway, Ireland.

## Benefits of nanoscale electrodes

The reasons why nanoscale electrodes might be of interest are now discussed.

The primary reason for use of ultramicroelectrodes and smaller electrodes is the benefit obtained from the enhanced mass transport which takes place.<sup>1–6</sup> As electrodes decrease in size, radial (3-dimensional) diffusion becomes dominant and results in faster mass transport. This high rate of mass transport (diffusion) at small electrodes enables measurement of kinetics by steady-state experiments rather than by transient techniques. In principle by decreasing electrode size from micrometre to nanometre scale, study of faster electrochemical and chemical reactions should be possible. This is because the electron transfer process is less likely to be limited by the mass transport of reactant to the electrode surface at very high rates of mass transport.<sup>9–11</sup>

However corrections for double-layer effects at tiny electrodes must also be considered.<sup>12,13</sup> From a fundamental viewpoint, what happens to diffusion-controlled currents at electrodes, as the size of the molecule, the diffusion distance and the thickness of the electrical double layer all become equivalent, must be considered. When molecular diffusion occurs within the electrical double layer at an electrode surface, the molecules experience solution characteristics different from those of the bulk solution, *e.g.* viscosity is increased. Such ideas can be probed by using nanoscopic electrodes: the diffusion layer becomes thinner as the electrode dimension becomes smaller, meaning that at very small electrodes the effects of the double layer viscosity should be apparent in the experimentally-recorded diffusion-controlled currents.<sup>12,13</sup>

Another motivation for the development of nanoscale electrodes is their use in a spatial scanning mode for electrochemical mapping of surfaces and interfaces. This technique, scanning electrochemical microscopy (SECM),<sup>14,15</sup> is dependent on the size of the scanned electrode for resolution. Microelectrodes offer a certain degree of performance which is well-established; however use of nanoelectrodes should enable greater spatial resolution.<sup>16–18</sup> For imaging, the probing electrode moving up to and across the probed surface must be of comparable size to any features which are to be imaged. Thus nano-sized surface features, maybe on a membrane or a corroding surface, require a nanosized probe in order to image that feature. This could lead to advances in areas such as nanobiotechnology and molecular biology. For example, imaging and activity measurements on individual biological assemblies, whether *in vivo* or *in vitro* could benefit greatly from the availability of nanoscale resolution with the SECM. Imaging of enzyme arrays and other bioactive sites at the nanoscale opens up possibilities for assessing and measurement of biological function at the individual molecule scale.

Analytical measurement systems can potentially exploit the increased mass transport characteristics of nanoelectrodes in achieving shorter response times to freely-diffusing species in solution (manifested perhaps as a shorter time to reach maximum signal in a constant potential amperometry set-up, or shorter deposition time requirement in a stripping voltammetry experiment). Another analytical benefit should be the increased faradaic to charging current ratio obtained, due again to the enhanced mass transport for diffusion-controlled faradaic currents.

Due to the extreme smallness of the active regions of nanoelectrodes, it should in principle be possible to pack many many nanoelectrodes onto a given footprint of a sensor device. The smaller the active electrode surface, the more of these can be constructed within the allotted area of a sensor system or other measurement device. This enables a far greater number of interaction points between the measurement system and the

matrix under examination as well as providing great scope for the realisation of massively parallel measurements. Individually-addressable nanoelectrodes can be achieved in principle. Robustness can be built into the sensor system based on redundancy as achieved for arrays of conventionally-sized sensors together with replication experiments, based on the ability to perform repeated experiments on multiple identical electrodes. Thus the many-electrode nanoarray can have individual sensors poised at different potentials, coated with different layers or even located within different regions of a sample matrix (*e.g.* fluid stream) in order to detect and pick-up different nuances of the sample matrix being investigated.

Finally the creation and study of certain types of nanoelectrodes and nanopores takes inspiration from biological membrane ion channels. Thus emulation of such biological processes can lead not only to novel sensor systems but also to an understanding of the biological function.<sup>19–21</sup>

An obvious challenge to successful exploration of the above benefits of nanoelectrodes is their fabrication and handling; another is the sensitivity of the instrumentation available with which to make reliable electrochemical measurements. This instrumentation problem can be circumvented by the use of nanoelectrode arrays or ensembles, whereby the individual electrodes in the array operate in parallel thus amplifying the signal while retaining the beneficial characteristics of the nanoelectrodes.

## Nanoelectrode fabrication

One of the greatest challenges facing nanoelectrode researchers is the preparation and fabrication of devices in order to study and realise some of the benefits discussed above. This aspect has been the most studied topic in this area over the last 15 years or so. There have been three main approaches:

- (i) Nanoband electrode fabrication by use of sputtered or evaporated metal films, exposed to the solution by their edge rather than their planar surface;
- (ii) The electrochemical etching of thin wires down to a cone shape followed by the insulation of all but the very tip of the cone with a suitable material;
- (iii) The deposition of metallic layers through nanoporous polymeric membranes.

The first two approaches provide individual nanoscale electrodes while the third provides arrays or ensembles of nanoelectrodes.

Nanobands were the first types of nanoelectrodes produced.<sup>12,13</sup> In principle they are easier to produce than nanodisc devices and did lead to the discovery of unusual/unexpected behaviour which is now the topic of further investigations. White and co-workers prepared nanoband electrodes in the 1980s. They wanted to study the inoperability of diffusion equations and the influence of near surface fluid properties (density, viscosity) on electrochemical behaviour when the electrode, the diffusion layer and the molecule undergoing electrolysis have similar dimensions. Platinum metal films of thicknesses between 2 and 100 nm were prepared by sputtering onto cleaved mica surfaces. After covering the Pt film with epoxy and fixing it within a tube, the end perpendicular to the Pt film was ground down to reveal the nanoband. Nanoband arrays were obtained by use of lithographic techniques<sup>22–24</sup> commonly used for microfabrication of electronic circuits and other microdevices. Gold was deposited onto glass, covered with silicon nitride, and then portions of the nitride and gold multilayers were etched away to leave islands of the multilayer structure. The metal (gold) edge exposed at the sides of these stacks served as nanoband electrodes, with widths of the order of 37 nm reported.

For many practical studies, nanoband electrodes are

suitable; they offer scope for the development of parallel nanoband electrode arrays for sensing applications. However a number of applications of nanoscale electrochemistry require disc or hemisphere electrodes, such as *in vivo* voltammetry and electrochemical imaging. For such applications, nanobands are not easily used.

The preparation of hemispherical nanoelectrodes with radii as small as 1 nm was introduced by Penner *et al.*<sup>9</sup> based on sequential electrochemical etching of microwires to a fine tip or cone and insulation of all but the very tip of the cone using a suitable insulator. This method is an adaptation of the previously used method for the preparation of conducting tips for scanning tunnelling microscopy (STM) when applied in liquid environments. In such cases the STM tip must be insulated in order to prevent the unwanted faradaic currents which occur when the scanning probe is biased *versus* the conductive substrate being imaged. Table 1 summarises the electrodes prepared with this etching/insulation method, showing the electrode materials, the etching methods and insulation materials used, and the sizes of the nanoelectrodes achievable (as given by their effective radii).

Penner *et al.*<sup>9</sup> etched PtIr alloy or Pt wires down to a tapered tip (cone). The etching was carried out electrochemically in a mixture of sodium hydroxide (2 M) and potassium cyanide (6 M) while applying a 25 V alternating current (ac) signal relative to an inert graphite counter electrode. The tapered tip was then pushed through a molten glass bead to insulate most of the cone, but not the very tip of the taper. Both the temperature of the molten glass and the rate at which the tip was pushed through were influential in the resultant aperture sizes created in the glass. The aperture in the glass exposed the tip of the cone to the solution in which the device is immersed, thus the glass aperture defined the size of the nanoelectrode achieved. Although the smallest aperture electrodes could not be visualised by scanning electron microscopy (SEM), they still portrayed an electrochemical signal characteristic of a cone (assumed to be equivalent to a hemisphere) with very small dimensions.

Bard and co-workers<sup>11</sup> used a slightly different approach when preparing Pt nanotips for SECM. They used Apiezon wax as the insulating material; however they completely covered the tip so that it was insulated when tested under voltammetric conditions. An aperture in the wax was then opened by applying a 10 V bias between that insulated tip and a conducting substrate. This opened up a pore in the wax at the point of closest proximity to the substrate and the tip was then amenable to study by voltammetry and SECM.

Unwin and co-workers<sup>16,17</sup> introduced the use of electrophoretically-deposited paints to insulate the tip. Either

cathodic or anodic deposition of paints can be employed. Post-painting heat treatment is required in order to shrink the paint and force the tip of the etched metal cone to protrude. This approach has been taken up by others<sup>25,27,28</sup> as well as subjected to further improvements in the painting procedure.<sup>29,30</sup> As can be seen from Table 1, this approach enables some really small electrodes to be manufactured (sub-nm up to 100's of nm) and is presently the most widely used approach to achieving ultrasmall electrodes on a one-off basis for fundamental studies. The size of the coating is controllable by the number of electrophoretic painting/heat treatment cycles used: the more painting/heat treatment, the smaller the apparent nanoelectrode dimensions. It is also low cost, using apparatus that is commonly available in electrochemistry laboratories. All that is needed other than regular electrochemical apparatus is the ac voltage supply.

This etching/insulation approach, however, produces cone electrodes which are approximated by a hemisphere in their electrochemical characterisation. An elegant improvement of this method was the addition of a post-insulation electrochemical etching of the metallic tip in order to produce a disc nanoelectrode.<sup>31</sup> In this case the etching and partial insulation of the cone tip was carried out, but then the exposed nanoelectrode was subsequently electrochemically etched down to a disc-shaped feature.

Other approaches to the preparation of individual nanoelectrodes have been described by various workers. Wong and Xu<sup>32</sup> described a process based on pyrolysis of methane as it is forced through a capillary. Under such circumstances the pyrolysed hydrocarbon results in a carbonaceous deposit on the internal walls of the capillary. Prolonged pyrolysis resulted in formation of a carbon deposit at the end of the capillary, to which electrical connection was made from the inside of the capillary. Such carbon deposits functioned well as nanoelectrodes, having effective radii in the region of 320 nm and 740 nm. Mirkin and co-workers<sup>33</sup> prepared nanoelectrodes by pulling glass capillaries containing sealed microwires using a commercially-available laser pipette puller; the pulling of the heated glass resulted in a narrowing of both the glass and the wire within. Both the thickness of the eventual wire and its glass surround can be manipulated by controlling the conditions during the pulling procedure. This strategy was further optimised by Schuhmann and co-workers,<sup>34</sup> who provide complete experimental details for the procedure (see Fig. 1 for a summary). In summary, the pipette puller uses a laser for the finely-controlled local heating of the glass and its internal microwire. Once heated the glass-wire composite is then pulled to drastically reduce both the radius of the wire and of the

**Table 1** Nanoelectrodes prepared by electrochemical etching of wires followed by partial insulation

Electrode material	Etching conditions	Tip insulation material	Nanoelectrode dimensions (effective radius).	Reference
PtIr	NaOH (2 M), KCN (6 M), 25 V ac	Glass	1.6 nm → μm	9
PtIr	CaCl <sub>2</sub> , HCl, H <sub>2</sub> O, 25 V ac	Apiezon wax, electrical breakthrough to expose tip	A few nm and up	11
Pt	NaNO <sub>2</sub> (sat'd), 1.2 V ac	Electrophoretic paints (anodic and cathodic) + heat treatment	<i>r</i> = 13 nm, 49 nm, 120 nm, 1.2 μm	16
Pt	NaCN (6 M) or CaCl <sub>2</sub> (50% v/v in H <sub>2</sub> O), 5 V ac	Electrophoretic (anodic) deposition of poly(acrylic acid) paint	<i>r</i> = 2–150 nm	25
Pt	CaCl <sub>2</sub> (50% v/v), HCl (25% v/v), H <sub>2</sub> O (25% v/v), 2 V ac	Polyimide (thermopolymerisation)	A few hundreds nm	26
Pt	NaNO <sub>2</sub> (10 M), 1.6 V ac	Electrophoretic (anodic) deposition of poly(acrylic acid) paint	<i>r</i> = 1.3 nm and up	27
Ag	NH <sub>4</sub> OH (35%) diluted 6 : 1 with water, 4.0 V dc	Cathodic electrophoretic paint + heat treatment	<i>r</i> = 50 nm, 70 nm, 2.6 μm	17
C fibre	NaOH (0.1 M), 4–5 V ac	Cathodic electrophoretic paint (inverted deposition) + heat treatment	<i>r</i> = 0.3 nm, 0.9 nm, 16 nm, 38 nm, 160 nm	29,30
Au	HCl (3.6 M), 1.7 V dc	Nail varnish containing nitrocellulose; post insulation pulse etching to produce flat nanoelectrode surface	<i>r</i> = 50–250 nm	31

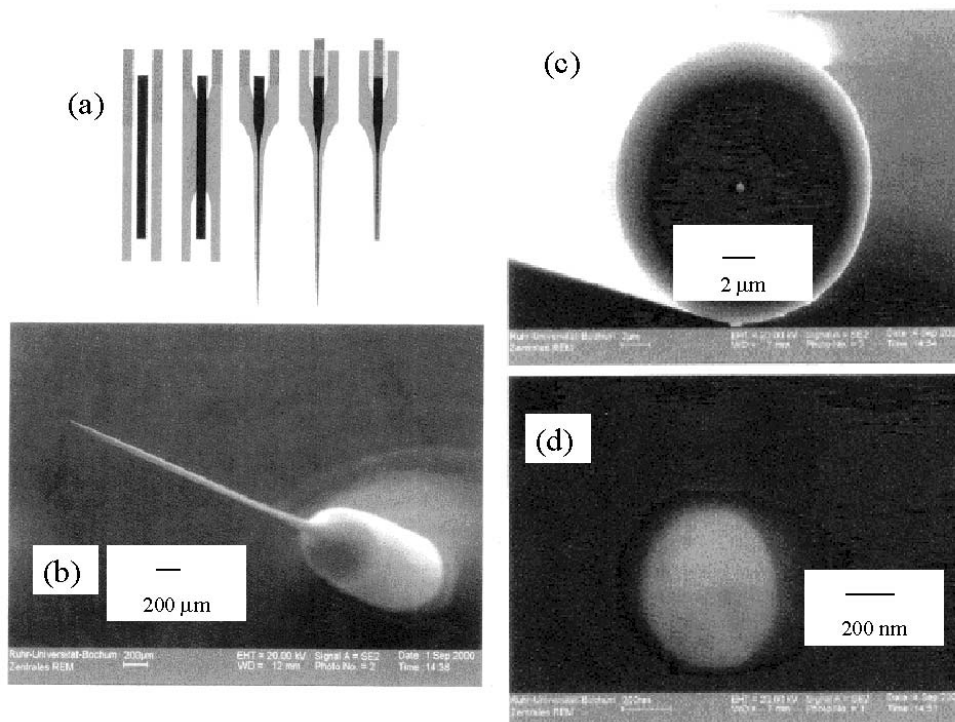


**Fig. 1** Fabrication sequence summary (a) for Pt nanodisc electrodes by the pipette pulling technique. (b) SEM image of a needle nanoelectrode. (c) SEM image of front end of a nanoelectrode. (d) Close-up of the Pt nanodisc (located at the end of the needle shown in (b)). Reproduced with permission from ref. 34.

glass, also providing a close-fitting seal between the glass and the metal wire. Using this method, each capillary-microwire section produces two nanodisc electrodes. After polishing, discs of diameters down to 10 nm were achieved.<sup>34</sup> This approach appears to offer a more systematic methodology as well as polishable nanoelectrode surfaces, unlike the etching/insulation approach discussed above. Thus these nanodiscs could be reused, which is an important aspect. Fig. 1 also displays some SEM images of both the needle-type electrode as well as close-up images of the metal nanodisc at the end of the needle, with its glass surround.

Individual nanoscale electrodes have their uses but their predominant disadvantage, aside from the difficulty of fabrication, is in the extremely small current which can be achieved with them. Thus there has been much interest in the development of collections of nanoelectrodes which operate in parallel. If this collection is arranged in an ordered manner with a controlled inter-electrode spacing, they are referred to as arrays; if the collection is not so ordered and there is not specific control over the inter-electrode spacing, then they are referred to as ensembles.

Nanoelectrode ensembles (NEEs)<sup>35</sup> have been the subject of investigation by Martin and co-workers.<sup>36,37</sup> They have prepared disc arrays by the electrodeposition of metals within the micrometre- and sub-micrometre-sized pores of polymeric porous membranes, referred to as the template synthesis method. These membranes are commercially available and are typically neutron-track-etched polycarbonate materials. The pores run right through the membrane. By sputtering a metal film onto one side of the membrane, that metal film can then be used as the electrode for subsequent electrodeposition into the pores. The smallest disc size achievable with that method was 200 nm diameter. By use of an electroless deposition process with membranes having pores of 30 nm and 10 nm diameters, successful achievement of the NEE was possible.<sup>37</sup> With electroless deposition, the surface onto which the metal is deposited does not need to be conductive. The chemistry of the

process has been reported in detail by Menon and Martin<sup>37</sup> and involves treatment of the surface of the pores with a sensitizer ( $\text{Sn}^{2+}$ ); this is then reacted with silver, to produce silver metal which is deposited on the pore surface; upon placing this into a gold plating bath, the silver is galvanostatically replaced by gold which then becomes an active site for the catalytic oxidation of formaldehyde with concurrent reduction of Au(I) to Au(0). This process continues within the pores resulting in deposition of gold nanowires as well as onto both sides of the membrane. The gold coating can later be removed from one side of the membrane to reveal the NEE formed from the ends of the wires within the nanopores. After suitable arrangement into a testable configuration, allowing electrical contact *etc.*, the NEEs prepared by this route were shown to have significant electroanalytical properties.

Another approach to NEEs was that of colloidal nanoparticle assembly.<sup>38</sup> Mica surfaces were functionalised with (3-mercaptopropyl)trimethoxysilane, producing a surface with thiol groups available for binding to a suitable metal; then gold nanoparticles were bonded to the surface. These NEEs were of course not uniform and behaved as expected for closely spaced electrode sites in a matrix (see later).

A further approach to NEEs is to insulate a planar electrode and then open up holes in that insulation layer through to the underlying electrode. Baker and Crooks<sup>39</sup> have developed a technique based on etching of alkane thiol self-assembled monolayers (SAMs) from a gold surface, producing NEEs which can be characterised both by electrochemistry and scanning probe microscopy, with radii of individual electrode elements as small as 6 nm. The preparation procedure employs single crystal gold coated with a monolayer of underpotentially-deposited (UPD) copper atoms. The thiol chemisorption takes place on top of this Cu UPD layer; finally the nanoelectrodes are produced by electrochemically etching to enlarge native defects in the thiol SAM using cyanide solution. Another SAM-based approach has been suggested.<sup>40</sup> In this case the active nanoelectrodes are actually redox species

anchored at the ends of alkane thiol SAMs: each redox-active molecule functions in the same way as an individual nanoelectrode.

On the other hand, Jeung *et al.*,<sup>41</sup> who also used the planar electrode coated with insulator approach, used block copolymer self-assembly to produce ordered arrays of pores on the electrode surface. The pores mediated the transport of electroactive species to the underlying electrode surface thus enabling the system to perform as a nanoelectrode array (NEA). In this case, the pores were at regular distances from each other. The insulating layer was a spin-coated polystyrene (PS)/polymethylmethacrylate (PMMA) mixture on a metallic substrate. This was then annealed in an electric field in order to structure the PMMA nanopores perpendicular to the planar electrode surface. Finally, UV treatment was used to crosslink the PS while destroying the PMMA, leaving the nanoporous self-assembled surface layer in place. This approach obviously produces nanopore arrays; the dimensions of the pores were 14 nm in diameter, with a 24 nm pore-to-pore spacing.

Myrick and co-workers<sup>42,43</sup> have reported two approaches for the preparation of recessed nanoelectrode arrays, based on the template synthesis method of Martin,<sup>36,37</sup> actually producing NEEs rather than NEAs. Commercially-available membranes with 200 nm diameter pores arranged in a hexagonal configuration were employed. Copper was first deposited onto one side of the membrane, followed by electrodeposition of gold through the pores. Finally the copper was removed, revealing an array of recessed nanoelectrodes.<sup>42</sup> In the other approach from the same group<sup>43</sup> they created shallower recesses using electrochemical gold stripping and/or ion bombardment gold stripping. Such nanowell electrodes were prepared with measurement of molecular electronic properties in mind.

Finally, carbon nanotubes (CNTs) have received much attention from an electroanalytical and sensing viewpoint.<sup>8,44,45</sup> However such assemblages tend to be bulk "forests" rather than any array with controllable inter-tube separations and the electrochemistry is not different from a regular-sized disc electrode. But in contrast to that, Koehne *et al.*<sup>46</sup> have recently reported the fabrication of NEAs prepared from CNTs in which, by combination with micro-lithography, it was possible to prepare NEAs with extremely low density of sites (*i.e.* of individual CNTs). Such low density offers advantages to electroanalysis as it incorporates the enhanced mass transport to each CNT in the array while also having a lower charging current. Fig. 2 illustrates the

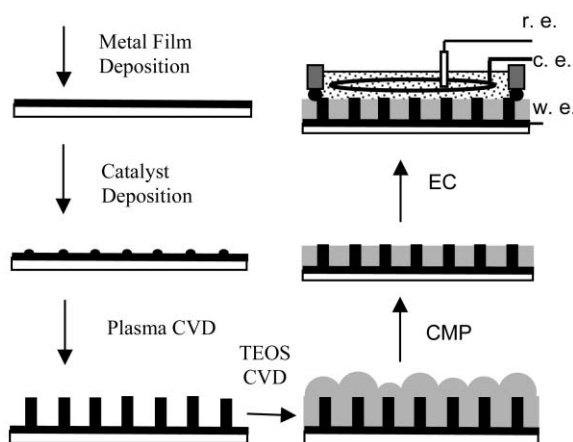


**Fig. 2** Summary of the fabrication of nanoelectrode arrays based on carbon nanotubes. Metal deposition = substrate film; catalyst = nickel catalyst pattern; plasma CVD = chemical vapour deposition (CVD) of CNTs; TEOS CVD = thermal CVD deposition of tetraethylorthosilicate, forming the SiO<sub>2</sub> film; CMP = chemical mechanical polishing to planarise the surface; EC = electrochemical testing set-up. Reproduced with permission from ref. 46.

fabrication process. The space between individual CNTs can be filled with a suitable insulator material such as silicon dioxide. The important point here is that the CNT–CNT spacing is open to control and thus the electrochemical properties can be manipulated. Thus well-ordered arrays and even NEEs can be achieved, if desired. The fabrication method is based on the growth of CNTs at nickel catalyst sites across the surface. Thus the arrangement of catalyst deposits is what controls the geometry of the eventual CNT NEA.<sup>46</sup> The radii of individual CNTs in this array were 17 nm, while the average inter-CNT spacing was 1.3 μm for the low-density NEA.

This latter strategy is the most technologically advanced approach to fabrication of NEAs so far reported. It offers opportunities for exploration of analytical/sensor applications in a number of areas.

## Electrochemistry at nanoelectrodes

The electrochemical study of nanoelectrodes and nanoelectrode arrays is important from a characterisation as well as possible application perspective. Around the time that interest in fabrication and evaluation of nanoscale electrodes started, around a decade and a half ago,<sup>9,11–13</sup> imaging technology was not capable of allowing the experimenter to "see" the nanoelectrode which had been prepared. It was not possible to see the tips of such electrodes using SEM thus the electrochemical response was used to infer the dimensions of the surface. The investigator was thus dependent totally on the electrochemical signal which was obtained and how that was related to the electrode dimensions, typically the radius.

Due to the small size of the nanoelectrodes, they exhibit a fast (three-dimensional) diffusion field and produce steady-state voltammograms (*i.e.* sigmoidal shape). This voltammogram shape is independent of the nanoelectrode geometry. Generally the nanoelectrode critical parameter, radius of the disc for example, is extracted by applying a suitable model for the steady-state current. Fig. 3 illustrates the possible diffusion modes and the corresponding steady-state current (limiting current) equations for hemisphere, inlaid disc<sup>1–6</sup> and recessed disc electrodes.<sup>47</sup>

Based on the fabrication procedures discussed above for preparation of individual nanoelectrodes, the nanoelectrodes which are prepared by the etching/partial insulation approach produce nanocones and have been approximated by the hemisphere model. The recessed disc model<sup>47</sup> has been

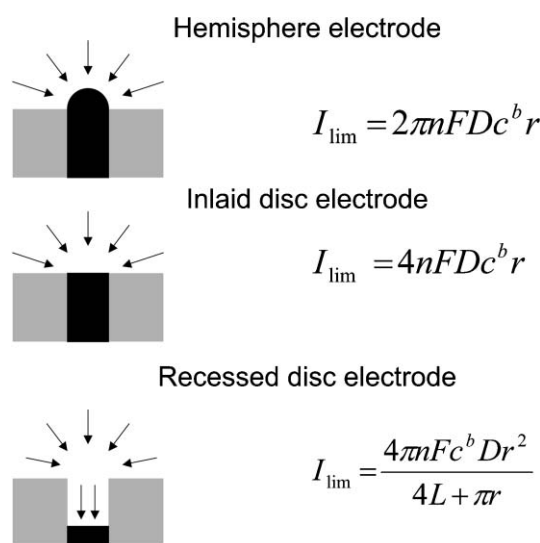


**Fig. 3** Nanoelectrode geometries: hemispherical electrode, inlaid disc electrode and recessed disc electrode; diffusion modes to these and the equations for the corresponding steady-state currents.

**Table 2** Steady-state voltammetric characterisation of nanoelectrodes

Electrode material	Model assumption	Redox probe species employed	Effective radius	References
Pt	Hemispherical electrode	Fe <sup>2+</sup> , Ferrocene, Ru(NH <sub>3</sub> ) <sub>6</sub> <sup>3+</sup>	≥ 1.6 nm	9
Pt	Hemispherical electrode	Fe(CN) <sub>6</sub> <sup>4-</sup>	13 nm–1.2 μm	16
Pt	Inlaid disc electrode	Ru(NH <sub>3</sub> ) <sub>6</sub> <sup>3+</sup>	10–900 nm	34
Pt	Recessed disc electrode	[(Trimethylammonio)methyl]ferrocene	10–20 nm	48
Ag	Hemispherical electrode	Ru(NH <sub>3</sub> ) <sub>6</sub> <sup>3+</sup>	50 nm–2.6 μm	17
Au	Inlaid disc electrode	Fe(CN) <sub>6</sub> <sup>4-</sup>	50–250 nm	31
C	Hemispherical electrode	Fe(CN) <sub>6</sub> <sup>3-</sup>	0.3 nm–160 nm	29,30
C	Hemispherical electrode	Dopamine	320 nm	32

employed to characterise nanoelectrodes deliberately prepared with a wax sheath surrounding and extending beyond the electrode surface, *i.e.* recessed nanoelectrodes.<sup>48</sup> Nanoelectrode papers generally refer to the apparent or effective radius ( $r_{app}$ ,  $r_{eff}$ ) of the nanoelectrode, since there is an assumption about the actual shape and the mode of diffusion governing transport to that electrode. Table 2 summarises some of the steady-state voltammetric characterisation of nanoelectrodes and the parameters of the electrode obtained from that analysis. As can be seen, many electrodes are characterised by the hemisphere electrode model, justified on the basis that the etching/coating procedures used produce cone electrodes which can be approximated by a hemisphere. Woo *et al.*<sup>31</sup> showed an interesting switch from hemisphere to inlaid disc behaviour using their additional etching procedure to remove the protruding cone. It should be noted that the voltammetric properties of nanoelectrodes agree with classical diffusion theory for nanoelectrodes of effective radii > 10 nm; below this limit there is a deviation from theory. However the microscale models have still been applied for the estimation of extremely small electrode radii, substantially less than 10 nm.

The steady-state voltammetric characterisation of nanoelectrodes is carried out with a redox-active species known to have fast electrode kinetics; for example, ferrocene in non-aqueous media, hexamminoruthenium(III) or hexacyanoferrate(III/II) in aqueous media have been used, with an excess of supporting electrolyte in all cases. Fig. 4 shows typical examples of steady state voltammetry at individual nanoelectrodes, in this case an etched carbon fibre coated with electrophoretic paint.

Watkins *et al.*<sup>25</sup> proposed that electrode surface areas for these very small devices can be assessed by measurement of the charge associated with the oxidation of a known quantity of the species bis(2,2'-bipyridine)chloro(4,4'-trimethylenedipyridine)-osmium(II) previously adsorbed to the nanoelectrode surface. This method is based on the known monolayer saturation surface coverage of the adsorbate and its oxidation reaction. Measurement of the charge for that reaction then enables

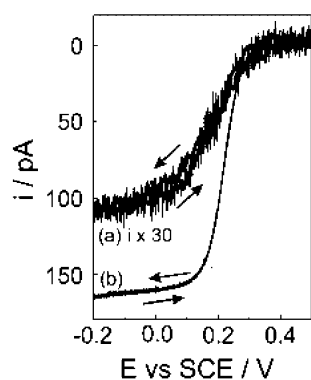


**Fig. 4** Typical steady state voltammograms for carbon fibre etched/electrophoretic paint insulated nanoelectrodes, as obtained in 0.01 M K<sub>3</sub>Fe(CN)<sub>6</sub> in 0.5 M KCl. Effective radii are calculated from the diffusion limited steady-state reduction currents as (a) 0.9 nm and (b) 38 nm. Scan rate 10 mV s<sup>-1</sup>. Reproduced with permission from ref. 29.

calculation of the real electroactive surface area. It was found that this method was in agreement with radii obtained by steady-state voltammetry assuming a hemispherical electrode. Deviations from this agreement were indicative of non-ideal electrode geometry.<sup>25</sup>

SECM has also been used for the characterisation of nanoelectrode shapes, based on the use of approach curves.<sup>11,33</sup> In this experiment, the probe electrode is poised at a potential in which a diffusion-controlled reaction for the redox-active species occurs. While maintaining that condition, the probe electrode is gradually moved closer to a surface. The current recorded at the moving electrode will then depend on both the shape of the approaching probe and on the conductivity of the surface. The exact shape of this current–distance curve (the approach curve) will depend on the geometry of the probe electrode. Thus the usual application of SECM can be switched from characterising the electrical/electrochemical properties of the surface to (using a known surface) characterising the geometry of the probe electrode. Bard and co-workers have applied this idea to the characterisation of cone nanoelectrodes as well as disc-shaped electrodes.<sup>11</sup>

Characterisation of NEEs and NEAs can be achieved by voltammetry of the same electroactive species and electrolyte solutions as used for single nanoelectrodes. Depending on the preparation procedures used, the same caution regarding application of different models for steady-state voltammetric behaviour apply. This is especially true for the lower extremity of the nanoelectrode range where imaging for shape and dimensions is not possible. Additionally, with NEEs and NEAs, the issue of diffusion regimes and whether they are independent for each electrode element of the array or whether they interact (overlap) must be considered.<sup>35–37,49</sup>

Fig. 5 illustrates the diffusional regime which may occur at NEEs and NEAs. The shape of the diffusion regimes will depend on the electrode dimensions, geometry, whether inlaid, recessed or protruding, and the separation between adjacent electrodes of the array. When the electrodes are sufficiently separated, each nanoelectrode of the nanoelectrode collective experiences its own diffusion regime, with independent radial (three-dimensional) diffusion to, for example, nanodiscs. However this is generally not the case for NEEs and they experience overlapping diffusion regimes such that one-dimensional diffusion dominates. The timescale (*e.g.* sweep rate in voltammetry) also influences the shape of the diffusion regime. For example, at an inlaid NEE, at short times (fast sweep rates) one-dimensional diffusion to each nanoelectrode can occur, resulting in peak-shaped cyclic voltammograms. At long times (slow sweep rates) the diffusion regimes to each nanoelectrode overlap, culminating in one-dimensional diffusion and resulting in peak-shaped voltammograms. At intermediate sweep rates, three-dimensional diffusion to each nanoelectrode in the ensemble occurs, and steady-state voltammograms are obtained. The timescales involved in the switching between the different behaviours depends on the size of the individual elements in the NEE as well as on the average electrode–electrode separation. A similar behaviour can occur

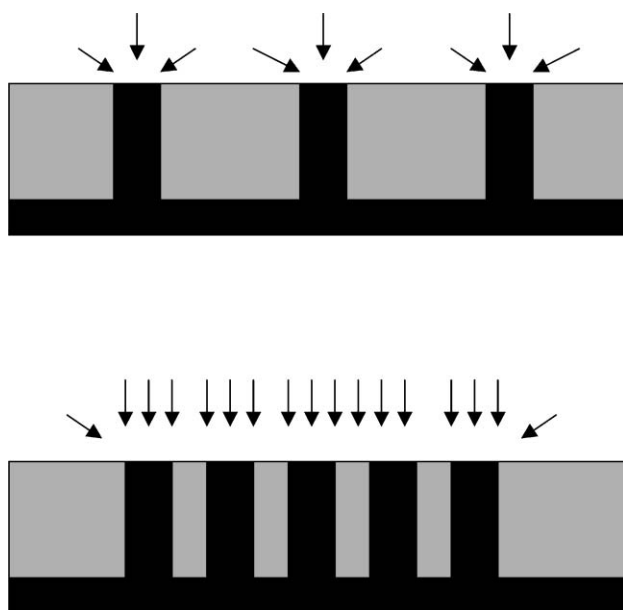


**Fig. 5** Diffusion to nanoelectrode arrays or ensembles: upper: individual diffusion regimes to each electrode of the array; lower: overlapping diffusion regimes, leading thus to one-dimensional diffusion.

at NEAs, but in this case the spacing between the elements of the array is more controlled and only steady state voltammetry will be obtained at anything but the fastest sweep rates. Fig. 6 illustrates typical voltammetric responses for two CNT arrays,<sup>46</sup> one high density in which the diffusion fields overlap to produce a peak-shaped voltammogram, and the other low-density, in which the diffusion regimes do not overlap and a steady state voltammogram is obtained.

An important consideration in the electrochemistry of NEEs and NEAs is the background or charging current.<sup>35</sup> This is proportional to the total geometric area of the electrode elements. However the diffusion-controlled current, when the sweep rate and interelectrode distance are such that the diffusion regimes at the electrodes overlap, will be proportional to the total area of the ensemble or array (*i.e.* active electrode surface as well as interelectrode insulation). This means that an effective enhancement of the signal (diffusion-controlled current) to noise (background, or charging current) ratio is obtained. This represents an important advantage to the analytical use of NEAs and NEEs.

## Applications

Applications of nanoelectrodes and ensembles or arrays of these are now summarised in three areas: physical electrochemistry, imaging science and analytical science.

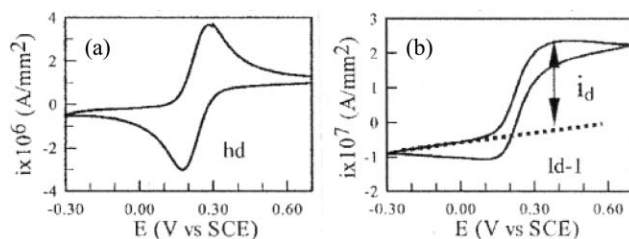


**Fig. 6** Cyclic voltammetric responses at CNT NEAs, (a) high density electrode, (b) low density array. 1 mM  $\text{K}_4\text{Fe}(\text{CN})_6$  in 1 M KCl. Scan rate  $20 \text{ mV s}^{-1}$ . Adapted with permission from ref. 46.

## Physical electrochemistry

Physical electrochemistry has been the main driving force for the establishment of reproducible and robust methods for the preparation of nanoelectrodes. The reason is that small electrodes enjoy enhanced mass transport rates (diffusion) and thus can be used to measure the kinetics of faster electrode reactions. However caution must be applied in such studies, as the electrodes are not necessarily what they seem<sup>50,51</sup> leading to errors in the kinetic measurements.<sup>52</sup> In early studies with nanoelectrodes it was observed that when electrode dimensions approach molecular size then known diffusion principles cease to be relevant because of changes in solution properties (viscosity, density) when the diffusion layer is as thick as (or even thinner than) the electrical double layer.<sup>12,13</sup> The influence of this on measured mass transport-limited currents at nanoelectrodes has been investigated by a number of groups, especially those of White<sup>27,28</sup> and Kucernak.<sup>29,30</sup>

In a number of recent papers from these groups, studies of electrode reactions at nanoelectrodes (Pt and C) both in the presence and absence of added electrolyte have shown that electrochemistry at such small electrodes becomes dominated by double layer effects and the potential of zero charge of the electrode relative to the formal potential of the redox species under study. Thus enhanced or diminished currents, relative to theoretical predictions based on classical diffusion models, are recorded at the smallest electrode depending on whether the redox species is anionic or cationic.<sup>28,30</sup>

## Imaging science

Applications of nanoelectrode probes in SECM is driven by the need to be able to map electrochemical activity of surfaces *etc* at greater resolution than is possible by micrometre sized scanned electrodes. Although various groups used SECM as a method for characterisation of new nanoelectrodes, Unwin's group<sup>17</sup> was the first to use them for imaging; for example, in the imaging of  $\text{Cl}^-$  diffusion from a  $50 \mu\text{m}$  pore (unfortunately, the dimension of the probe electrode used in the imaging was not specified).

Schuhmann and co-workers<sup>18</sup> have used Pt nanodisc electrodes prepared by the pipette-pulling method<sup>34</sup> for the imaging of microfabricated structures. The microstructure used as the test sample for imaging, was produced by the LIGA technique (LIGA is a microfabrication technique which combines lithography, electroplating and moulding, the acronym comes from the German words for this: lithographie, galvanoformung, abformung) and consisted of a three-dimensional structure of hexagonal holes. The imaging was performed in amperometric mode, using  $\text{Ru}(\text{NH}_3)_6^{3+}$  as redox-active species. This functions by diffusing through the microstructure towards the probe nanoelectrode where the change in current related to the distance diffused is a measure of surface distance from the probe. Very clear benefit in the imaging of this structure using a  $225 \text{ nm}$  radius probe electrode rather than the more traditional  $5 \mu\text{m}$  radius probe was presented.<sup>18</sup>

## Analytical science

Analytical applications of nanoelectrodes in their various forms have begun to emerge. Although not nanoelectrodes, Wong and Xu<sup>32</sup> used a  $1 \mu\text{m}$  C electrode and could achieve detection limits for dopamine of  $5.8 \times 10^{-7} \text{ M}$  and  $7.6 \times 10^{-8} \text{ M}$  by cyclic and square wave voltammetries, respectively; the corresponding figures at a conventionally-sized C electrode (typically mm diameter) would be  $10^{-5} \text{ M}$  to  $10^{-6} \text{ M}$ , thus offering some support for the analytical uses of ultrasmall electrodes. Similarly ultrasmall Pt electrodes were employed for glucose detection using immobilised glucose oxidase with a detection limit of  $20 \mu\text{M}$  and a response time of

2 s.<sup>53</sup> En route to development of a method for measurement of nanoelectrode surface areas, Watkins *et al.*<sup>25</sup> have demonstrated the detection of zeptomole ( $10^{-21}$  mol) quantities of an adsorbed redox species on a nanoelectrode surface, indicating that moving to very small electrode is not detrimental to detection of very small amounts of substance. However, definitive reports on analytical utility of nanoelectrodes have yet to appear.

A significant analytical challenge is that of single molecule detection (SMD). Achievement of this will enable various fundamental properties of isolated molecules to be studied, such as formal potentials, diffusion coefficients and kinetic parameters. Bard and co-workers<sup>48</sup> have exploited the ability of a recessed nanoelectrode to construct an extremely small-volume thin-layer cell, when the protruding electrode surround is brought up to contact with a conducting surface. One or more molecules is trapped within this volume as the tip is moved toward the surface. These electroactive molecules then diffuse back and forth between the electrode tip and the substrate as they are oxidised at *e.g.* the nanoelectrode and reduced at the conducting substrate surface.<sup>48</sup>

Koehne *et al.*<sup>46</sup> examined the ability of CNT NEAs to be used for detection of electroactive compounds in solution. Using arrays with a low spatial density of CNTs, so that they each had independent diffusion fields, they detected low nanomolar concentrations of electroactive species using differential pulse voltammetry. These CNT arrays were also employed for DNA sensing, illustrating the wide range of possible analytical applications for these sensor devices.<sup>46</sup>

Using NEEs fabricated by the template synthesis method, Martin and co-workers<sup>37</sup> have demonstrated the analytical capabilities of these devices. For example, using 10 nm diameter gold disc NEEs, the ability to detect concentrations was three orders of magnitude better (1.6 nM) than at a conventional (mm-sized) disc electrode (1.6  $\mu$ M).<sup>37</sup> This can be attributed to the low background (charging) current relative to the enhanced diffusion-controlled faradaic current at these NEEs. Extension into ionomer film modified NEEs enabled detection of analytes following ion-exchange preconcentration and yielded a detection limit of 1 nM for Ru(NH<sub>3</sub>)<sub>6</sub><sup>3+</sup>.<sup>54</sup> The direct determination of cytochrome *c* at gold NEEs was also possible, without the need for adding a surface-promoter in order to achieve the best electrochemical performance (0.03  $\mu$ M cytochrome *c*).<sup>55,56</sup>

## Nanopores

The above sections have been concerned with methods for the preparation and characterisation of nanoscale electrodes, where measurements of charge transfer are of interest, for whatever application. Of course nature has been adept at creating ultrasmall structures for different functions, including charge transfer. One set of such natural nanostructures are the membrane channel proteins.<sup>19,20</sup> Charge transfer through such nanochannels is widely studied, for example movement of DNA molecules through reconstituted membrane channels has been proposed as a means of analysing DNA.<sup>20</sup> In that case,  $\alpha$ -haemolysin channels were reconstituted in bilayer lipid membranes. This protein forms a channel 2.6 nm in diameter, large enough for one single stranded DNA or RNA molecule to pass. The passage of the large molecule can be detected as a decrease in ionic current due to passage of background electrolyte under the influence of an applied potential difference across the membrane.<sup>20</sup>

There have been a number of approaches to development and measurement of nanopores in a manner analogous to these natural ion-transport pores. Chang *et al.*<sup>57</sup> developed a silicon dioxide nanochannel of the order of 4.5 nm in diameter

through which DNA passage could be detected. Mara *et al.*<sup>58</sup> developed conical pores with a 4 nm smaller end and 2 micron wider end. DNA passage could be detected and discrimination between DNA fragments of differing lengths was possible. Tong *et al.*<sup>59</sup> prepared arrays of nanopores in silicon nitride, with a pore width below 10 nm achieved. Such devices could be utilised for size-exclusion separation processes. Various electrochemical studies on fabricated nanopore systems have been reported. Martin and co-workers<sup>21</sup> have been at the forefront of these developments. One such example was the idea that a nanopore within a membrane which separated two electrolyte solutions could be employed as a molecule counter.<sup>60</sup> Application of a constant transmembrane potential caused a current in the cell which was diminished when an ion which matched the pore diameter of the nanopore entered the nanopore, analogous to the DNA detection approach outlined above with the natural ion channel protein. Concentrations of model analyte ions as low as  $10^{-10}$ – $10^{-11}$  M could be determined using a nanopore of diameter 2.8 nm.<sup>21</sup> The availability of well-characterised nanopore membranes has fomented a resurgence in interest in particle counting by the Coulter method.<sup>61</sup>

Electrochemical studies of nanopore processes include the imaging of diffusion through single nanopores using combined SECM–atomic force microscopy (AFM).<sup>62</sup> Here 100 nm pore diameters in a polycarbonate membrane were imaged by detecting the movement of a redox-active species through the pores. This concept has recently been extended to the sensing of nanoparticles at nanopore membranes.<sup>63</sup> In this case, the movement of polystyrene nanoparticles through a track-etched polycarbonate membrane was detected using SECM.

Very recently, a single microelectrode located at the bottom of an inverted cone has been developed.<sup>64</sup> This has been referred to as a nanopore electrode, because the electrochemical response at the recessed electrode can be used to study mass transport through the opening at the top of the cone, which is smaller than that of the electrode. This can be thought of as a special case of the lagoon microelectrode.<sup>50,51</sup> The fabrication procedure involves electrochemical etching of a Pt microwire and completely sealing the resulting cone into a glass capillary. The shape of the etched wire in this case does not change when sealed into the glass. Finally the glass extending beyond the Pt etched wire is polished flat, very gently, with iterative voltammetric testing in redox-active analyte solution (to monitor when the tip of the Pt wire has been exposed by the glass polishing procedure). Then, to produce the recessed Pt electrode, the Pt is subjected to further electrochemical etching to cause the surface to retreat back within the glass.<sup>64</sup> This very simple procedure should have wide applicability for the *in situ* electrochemical study of nanopore processes.

Finally, the use of nanopore membranes at the interface between two immiscible electrolyte solutions (ITIES) for ion transfer voltammetry has been suggested as a simple strategy for the characterisation of nanopore membrane materials.<sup>65,66</sup>

## Conclusions and prospects

The topic of nanoelectrodes and arrays or ensembles of these has been summarised in this review. It can be seen that such devices offer advantages in a number of areas of investigation. The main achievements in recent times have been the development of reliable methods for the preparation of nanoelectrodes and NEEs/NEAs. Availability of these methods should open up the field to further study and development of novel applications. Although the etch and insulate approach to nanoelectrode preparation has become popular in recent years, it seems to this author that the use of heating and pulling of glass capillaries containing sealed-in microwires offers better scope for a more automated and reliable long-term approach to

nanoelectrode fabrication. This method has the advantage too of producing nanodisc shapes rather than the cones produced by etching. The template synthesis method for the preparation of nanoelectrode ensembles, by deposition into commercially-available nanoporous membranes, offers scope for simple preparation of devices for myriad investigations. However the low-density CNT NEAs offer a high technology route to array device fabrication which could be useful within both chemical sensor and biosensor developments.

Regarding applications, physical electrochemistry, imaging science and analytical science have been investigated so far, but there are many further areas for investigation especially within the study of the analytical scope of the different types of nanoelectrode discussed above. Although detection of model redox analytes at NEEs and CNT arrays has been demonstrated, application to real sample matrices and to more realistic target analytes must still be encountered. It remains to be seen, for example, whether surface-fouling by the non-electroactive components of many natural sample matrices will have a deleterious effect on the voltammetric responses at NEEs. NEAs consisting of low-density carbon nanotubes also offer considerable scope for investigations of further applications. Again, model redox probe molecules have been detected, as has demonstration of DNA analysis.

As with any experimental endeavour, the availability of the device preparation methods should open up the study and application of these systems to a wider scientific community. It is hoped that the present review will in some way help this broadening of possible applications within the analytical arena.

## Acknowledgements

The author thanks Science Foundation Ireland (02/IN.1/B84) and the European Commission (FP6-IST-1-508774-IP) for support.

## References

- R. M. Wightman and D. O. Wipf, in *Electroanalytical Chemistry*, ed. A. J. Bard, Marcel Dekker, New York, 1989, vol. 15, p. 267.
- A. M. Bond, *Analyst*, 1994, **119**, R1.
- R. J. Forster, *Chem. Soc. Rev.*, 1994, **23**, 289.
- C. G. Zoski, *Electroanalysis*, 2002, **14**, 1041.
- R. Feeney and S. P. Kounaves, *Electroanalysis*, 2000, **12**, 677.
- K. Stulik, C. Amatore, K. Holub, V. Maracek and W. Kutner, *Pure Appl. Chem.*, 2000, **72**, 1483.
- J. M. Elliott, G. S. Attard, P. N. Bartlett, J. R. Owen, N. Ryan and G. Singh, *J. New Mat. Electro. Syst.*, 1999, **2**, 239.
- M. Musameh, J. Wang, A. Merkoci and L. H. Lin, *Electrochem. Commun.*, 2002, **4**, 743.
- R. M. Penner, M. J. Heben, T. L. Longin and N. S. Lewis, *Science*, 1990, **250**, 1118.
- R. M. Penner, M. J. Heben and N. S. Lewis, *Anal. Chem.*, 1989, **61**, 1630.
- M. V. Mirkin, F.-R. F. Fan and A. J. Bard, *J. Electroanal. Chem.*, 1992, **328**, 47.
- R. B. Morris, D. J. Franta and H. S. White, *J. Phys. Chem.*, 1987, **91**, 3559.
- J. D. Seibold, E. R. Scott and H. S. White, *J. Electroanal. Chem.*, 1989, **264**, 281.
- M. V. Mirkin and B. R. Horrocks, *Anal. Chim. Acta*, 2000, **406**, 119.
- Scanning Electrochemical Microscopy*, ed. A. J. Bard and M. V. Mirkin, Marcel Dekker, New York, 2001.
- C. J. Slevin, N. J. Gray, J. V. Macpherson, M. A. Webb and P. R. Unwin, *Electrochem. Commun.*, 1999, **1**, 282.
- N. J. Gray and P. R. Unwin, *Analyst*, 2000, **125**, 889.
- B. Ballesteros Katemann, A. Schulte and W. Schuhmann, *Electroanalysis*, 2004, **16**, 60.
- T. A. van de Goor, *PharmaGenomics*, 2004, 28.
- J. J. Kasianowicz, E. Brandin, D. Branton and D. W. Deamer, *Proc. Natl. Acad. Sci. USA*, 1996, **93**, 13770.
- P. Kohli, M. Wirtz and C. R. Martin, *Electroanalysis*, 2004, **16**, 9.
- M. P. Nagale and I. Fritsch, *Anal. Chem.*, 1998, **70**, 2902.
- M. P. Nagale and I. Fritsch, *Anal. Chem.*, 1998, **70**, 2908.
- C. S. Henry and I. Fritsch, *J. Electrochem. Soc.*, 1999, **146**, 3367.
- J. J. Watkins, J. Y. Chen, H. S. White, H. D. Abruna, E. Maisonhaute and C. Amatore, *Anal. Chem.*, 2003, **75**, 3962.
- P. Sun, Z. Zhang, J. Guo and Y. Shao, *Anal. Chem.*, 2001, **73**, 5346.
- J. L. Conyers, Jr. and H. S. White, *Anal. Chem.*, 2000, **72**, 4441.
- J. J. Watkins and H. S. White, *Langmuir*, 2004, **20**, 5474.
- S. Chen and A. Kucernak, *Electrochem. Commun.*, 2002, **4**, 80.
- S. Chen and A. Kucernak, *J. Phys. Chem.*, 2002, **106**, 9396.
- D. H. Woo, H. Kang and S. M. Park, *Anal. Chem.*, 2003, **75**, 6732.
- D. K. Y. Wong and L. Y. F. Xu, *Anal. Chem.*, 1995, **67**, 4086.
- Y. Shao, M. V. Mirkin, G. Fish, S. Kokotov, D. Palanker and A. Lewis, *Anal. Chem.*, 1997, **69**, 1627.
- B. Ballesteros Katemann and W. Schuhmann, *Electroanalysis*, 2002, **14**, 22.
- P. Ugo, L. M. Moretto and F. Veza, *ChemPhysChem*, 2002, **3**, 917.
- R. M. Penner and C. R. Martin, *Anal. Chem.*, 1987, **59**, 2625.
- V. P. Menon and C. R. Martin, *Anal. Chem.*, 1995, **67**, 1920.
- W. Cheng, S. Dong and E. Wang, *Anal. Chem.*, 2002, **74**, 3599.
- W. S. Baker and R. M. Crooks, *J. Phys. Chem.*, 1998, **102**, 10041.
- S. E. Creager and P. T. Radford, *J. Electroanal. Chem.*, 2001, **500**, 21.
- E. Jeung, T. H. Galow, J. Schotter, M. Bal, A. Ursache, M. T. Tuominen, C. M. Stafford, T. P. Russell and V. M. Rotello, *Langmuir*, 2001, **17**, 6396.
- U. Evans, P. E. Colavita, M. S. Doescher, M. Schiza and M. L. Myricks, *Nano Lett.*, 2002, **2**, 641.
- M. S. Doescher, U. Evans, P. E. Colavita, P. G. Miney and M. L. Myricks, *Electrochem. Solid-State Lett.*, 2003, **6**, C112.
- S. Sotiropoulou and N. A. Chaniotakis, *Anal. Bioanal. Chem.*, 2003, **375**, 103.
- X. Yu, D. Chattopadhyay, I. Galeska, F. Papadimitrakopoulos and J. F. Rusling, *Electrochem. Commun.*, 2003, **5**, 408.
- J. Koehne, J. Li, A. M. Cassell, H. Chen, Q. Ye, H. T. Ng, J. Han and M. Meyyappan, *J. Mater. Chem.*, 2004, **14**, 676.
- A. M. Bond, D. Luscombe, K. B. Oldham and C. G. Zoski, *J. Electroanal. Chem.*, 1988, **249**, 1.
- F.-R. F. Fan, J. Kwak and A. J. Bard, *J. Am. Chem. Soc.*, 1996, **118**, 9669.
- J. C. Hulthen, V. P. Menon and C. R. Martin, *J. Chem. Soc., Faraday Trans.*, 1996, **92**, 4029.
- A. S. Baranski, *J. Electroanal. Chem.*, 1991, **307**, 287.
- K. B. Oldham, *Anal. Chem.*, 1992, **64**, 646.
- J. Chen and K. Aoki, *Electrochem. Commun.*, 2002, **4**, 24.
- S. Hrapoviv and J. H. T. Luong, *Anal. Chem.*, 2003, **75**, 3308.
- P. Ugo, L. M. Moretto, S. Bellomi, V. P. Menon and C. R. Martin, *Anal. Chem.*, 1996, **68**, 4160.
- P. Ugo, N. Pepe, L. M. Moretto and M. Battagliarin, *J. Electroanal. Chem.*, 2003, **560**, 51.
- L. M. Moretto, N. Pepe and P. Ugo, *Talanta*, 2004, **62**, 1055.
- H. Chang, F. Kosari, G. Andreadakis, M. A. Alam, G. Vasmatzis and R. Bashir, *Nano Lett.*, 2004, **4**, 1551.
- A. Mara, Z. Siwy, C. Trautmann, J. Wan and F. Kamme, *Nano Lett.*, 2004, **4**, 497.
- H. D. Tong, H. V. Jansen, V. J. Gadgil, C. G. Bostan, E. Berenschot, C. J. M. van Rijn and M. Elwenspoek, *Nano Lett.*, 2004, **4**, 283.
- Y. Kobayashi and C. R. Martin, *J. Electroanal. Chem.*, 1997, **431**, 29.
- R. R. Henriquez, T. Ito, L. Sun and R. M. Crooks, *Analyst*, 2004, **129**, 478.
- J. V. Macpherson, C. E. Jones, A. L. Barker and P. R. Unwin, *Anal. Chem.*, 2002, **74**, 1841.
- S. Lee, Y. Zhang, H. S. White, C. C. Harrell and C. R. Martin, *Anal. Chem.*, 2004, **76**, 6108.
- B. Zhang, Y. Zhang and H. S. White, *Anal. Chem.*, 2004, **76**, 6229.
- R. A. W. Dryfe and B. Kralj, *Electrochem. Commun.*, 1999, **1**, 128.
- M. Platt, R. A. W. Dryfe and E. P. L. Roberts, *Langmuir*, 2003, **19**, 8019.